

Primary Frequency Response in Capacity Expansion With Energy Storage

Miguel Carrión ^{1b}, *Member, IEEE*, Yury Dvorkin ^{1b}, *Member, IEEE*, and Hrvoje Pandžić, *Member, IEEE*

Abstract—Massive integration of renewable energy resources calls for new operating and planning paradigms, which address reduced controllability and increased uncertainty on the generation side. On the other hand, emerging energy storage technologies can provide additional flexibility. Therefore, generation and storage expansion models need to be coordinated to ensure sufficiency of system-wide response capabilities within different regulation intervals. This paper proposes a coordinated generation and storage expansion formulation considering primary frequency response constraints. This is a stochastic mixed-integer linear program solved using an off-the-shelf solver. The proposed formulation is compared to the case when primary frequency response is neglected. The case study performed for an eight-zone ISO New England test system quantifies the value of energy storage simultaneously providing primary frequency response and spatio-temporal arbitrage.

Index Terms—Energy storage, generation expansion, mixed-integer linear programming, primary frequency response, unit commitment.

NOTATION

Indices

- d Index of characteristic days.
- g Index of generating units (existing and candidate).
- j Index of candidate storage units.
- k Index of contingencies.
- ℓ Index of transmission lines.
- n Index of buses.
- t Index of time periods.
- ω Index of scenarios.

Sets

- D Set of characteristic days.
- G Set of generating units (existing and candidates).

- G_n Set of generating units (existing and candidates) connected to bus n .
- $G^{C,C}$ Set of candidate conventional generating units.
- $G^{C,I}$ Set of candidate renewable generating units.
- $G^{E,C}$ Set of existing conventional generating units.
- $G^{E,I}$ Set of existing renewable generating units.
- J^C Set of candidate storage units.
- J_n^C Set of candidate storage units connected to bus n .
- K Set of contingencies.
- L Set of transmission lines.
- L_n^O Set of transmission lines originating at bus n .
- L_n^F Set of transmission lines ending at bus n .
- N Set of buses.
- T Set of time periods.
- T_d Set of time periods on characteristic day d .
- T_d^O Initial time period of characteristic day d .
- T_d^L Last time period of characteristic day d .
- Ω Set of scenarios.

Variables

- c_{jd}^{Deg} Degradation cost of storage j in day d and scenario ω (\$).
- g_{gtw} Power generated by generating unit g during period t and under scenario ω (MW).
- g_g^{IN} Installed capacity of candidate conventional unit g (MW).
- g_{gtw}^{PC} Power generated by generating unit g during period t and under scenario ω in post-contingency state k (MW).
- g_{gtw}^{S} Power spilled by renewable unit g during period t and under scenario ω (MW).
- $p_{\ell tw}^{\text{L}}$ Power flow through line ℓ during period t and under scenario ω (MW).
- $p_{\ell tw}^{\text{L,PC}}$ Power flow through line ℓ during period t and under scenario ω in post-contingency state k (MW).
- p_{ntw}^{UD} Unserved demand at bus n during period t and under scenario ω (MW).
- $p_{ntw}^{\text{UD,PC}}$ Unserved demand at bus n during period t and under scenario ω in post-contingency state k (MW).
- s_{jtw} Energy stored in storage unit j at the end of period t and under scenario ω (MWh).
- s_{jtw}^{PC} Energy stored in storage unit j at the end of period t and under scenario ω in post-contingency state k (MWh).

Manuscript received December 5, 2016; revised May 30, 2017; accepted July 31, 2017. Date of publication August 7, 2017; date of current version February 16, 2018. The work of H. Pandžić was supported by the Croatian Science Foundation and Croatian TSO (HOPS) under the project Smart Integration of RENEwables SIREN (I-2538-2015). The work of M. Carrión was supported in part by the Ministry of Economy and Competitiveness of Spain through Project DPI2015-71280-R (MINECO/FEDER, UE). Paper no. TPWRS-01824-2016. (Miguel Carrión, Yury Dvorkin, and Hrvoje Pandžić contributed equally to this work.) (Corresponding author: Yury Dvorkin.)

M. Carrión is with the Universidad de Castilla-La Mancha, Toledo 45071, Spain (e-mail: miguel.carrión@uclm.es).

Y. Dvorkin is with the Department of Electrical and Computer Engineering, New York University, New York, NY 10003 USA (e-mail: dvorkin@nyu.edu).

H. Pandžić is with the Faculty of Electrical Engineering and Computing, University of Zagreb, Zagreb 10000, Croatia (e-mail: hrvoje.pandzic@iee.org).

Color versions of one or more of the figures in this paper are available online at <http://ieeexplore.ieee.org>.

Digital Object Identifier 10.1109/TPWRS.2017.2735807

$s_{jt\omega}^C$	Power charged into storage unit j during period t and under scenario ω (MW).	$U_{gt\omega}^I$	Available capacity of renewable (non-dispatchable) unit g during period t and under scenario ω (pu).
$s_{jt\omega}^D$	Power discharged from storage unit j during period t and under scenario ω (MW).	U_{gk}^{PC}	Binary parameter that is equal to 0 if outage of unit g is a contingency in post-contingency state k , and 1 otherwise.
$s_{jt\omega k}^{D,PC}$	Power discharged from storage unit j during period t and under scenario ω in post-contingency state k (MW).	V_{jk}^{PC}	Binary parameter that is equal to 0 if outage of storage unit j is a contingency in post-contingency state k , and 1 otherwise.
$s_j^{E,IN}$	Installed energy capacity of candidate storage unit j (MWh).	W_d	Weight of characteristic day d .
$s_j^{P,IN}$	Installed power capacity of candidate storage unit j (MW).	x	Unit lifetime (years).
$x_{gt\omega k}^{G,I}$	Auxiliary variable used to formulate the product of variables $z_{gt\omega k}^G$ and g_g^{IN} (MW).	X_ℓ	Reactance of line ℓ (pu).
$z_{gt\omega k}^G$	Binary variable being equal to 1 if the production of unit g is equal to its capacity during period t under scenario ω and in post-contingency state k , and 0 otherwise.	γ^{Degr}	Parameter used to limit the degradation cost of storages.
$\theta_{nt\omega}$	Voltage angle at bus n during period t and under scenario ω (rad).	γ_j^{EP}	Energy/power ratio of selected storage technology.
$\theta_{nt\omega k}^{PC}$	Voltage angle at bus n during period t and under scenario ω in post-contingency state k (rad).	γ_j^{min}	Minimum amount of energy that must remain in storage unit j to avoid premature aging (pu).
		γ_j^0	Energy stored in storage unit j at the beginning of the planning horizon (pu).
		π_ω	Probability of scenario ω .
		τ_k	Probability of contingency k .

Parameters

a	Capital recovery factor.
C_g^G	Generation cost of conventional unit g (\$/MW).
$C_g^{G,IN}$	Investment cost of candidate generating unit g (\$/MW).
$C_j^{\text{SE},IN}$	Energy investment cost of candidate storage unit j (\$/MWh).
$C_j^{\text{SP},IN}$	Power investment cost of candidate storage unit j (\$/MW).
C^{UD}	Cost of unserved demand (\$/MW).
$C^{\text{UD},PC}$	Cost of unserved demand after a contingency (\$/MW).
$D_{nt\omega}$	Power demand at bus n during period t and under scenario ω (MW).
D_g^G	Speed-governor droop of generating unit g (MW/Hz).
$F(\ell)$	Destination or receiving bus of line ℓ .
G_g^{IN}	Maximum capacity to be installed of candidate generating unit g (MW).
G_g^{max}	Maximum capacity of generating unit g (MW).
$G_g^{\text{up}}/G_g^{\text{dw}}$	Ramp up/down limit of conventional unit g (MW/h).
N_t	Duration of period t (h).
N_T	Number of periods.
N_j^{Cyc}	Maximum number of complete charge/discharge cycles of storage j .
M	Large enough parameter.
M^G	Large enough parameter.
M^S	Large enough parameter.
$O(\ell)$	Origin or sending bus of line ℓ .
$P_\ell^{L,\text{max}}$	Capacity of line ℓ (MW).
r	Interest rate.
$S^{\text{IE},\text{max}}$	Limit on overall installed storage capacity (MWh).

I. INTRODUCTION

LARGE-SCALE integration of renewable generation, such as photovoltaic and wind power resources, introduces additional uncertainty and variability on power system operation [1], thus imposing more stringent flexibility requirements [2]–[4]. These resources with limited dispatchability displace conventional fossil-fired units, thus reducing the available means to continuously maintain the generation-load balance. Even though renewable generation can be used for providing inertial and primary frequency response (PFR) [5]–[7], as well as active power reserve [8]–[10], the total amount of flexibility that they can provide does not fully make up for the displaced conventional units. Therefore, system operators seek to ensure sufficient flexible capacity to reliably operate large fleets of renewable generation via investments in ultra-flexible conventional units, e.g., gas-fired [11]–[14], and non-conventional technologies, e.g., energy storage [16], [17], [19], [20]. However, [11]–[14], [16], [17], [19], [20] focus on mitigating the impacts of the renewable integration within the secondary and tertiary regulation intervals, without ensuring sufficient PFR to withstand a major outage.

Recent measurement-driven studies have indicated that the available flexibility within the primary regulation interval, including PFR, has considerably reduced. For example, the system-wide PFR has reduced in the US Eastern Interconnection from 37.5 MW/mHz in 1994 to 30.7 MW/mHz in 2004 [21]. Furthermore, integration of renewable generation has been identified as the major cause of PFR scarcity observed during several severe contingencies registered in the WECC system [22]. Several enhancements to unit commitment and optimal power flow frameworks have been proposed to ensure PFR adequacy, [23]–[25]. These studies aim to schedule and dispatch the existing generation resources in a way that ensures sufficient PFR of the system at all times. On the other hand, these studies do not account for the ability of storage technologies to provide PFR

and do not guarantee long-term PFR adequacy necessary for planning studies. Several demonstration projects have validated the technical feasibility of energy storage as a PFR provider [26], [27]. Consequently, this paper develops a framework to assist system operators in co-planning generation and storage expansion to ensure PFR adequacy under high penetrations of renewable generation resources.

A. Literature Review

Energy storage is technically feasible for various power system applications [28], [29], including spatio-temporal arbitrage and congestion relief [16], [17], [19], [20], active power ancillary services [30], [31], inertial and PFR [31]–[34], and post-contingency corrective actions [35]. The value of services provided by energy storage depends on their location and size, which should be jointly optimized to harvest maximum benefits [16]. References [16], [17], [19], [20] describe optimization models for joint siting and sizing of distributed energy storage providing spatio-temporal arbitrage. However, these models do not explicitly account for credible contingencies and security constraints, thus neglecting the value of storage for contingency mitigation. References [33] and [34] focus on optimal energy storage sizing for providing PFR, but do not optimize its network placement, which may cause overloads when PFR is deployed.

Literature regarding co-planning of generation and storage expansion is thin. Reference [36] proposes an approach based on dynamic programming and gradient search to co-optimize a future generation mix and energy storage in transmission-unconstrained power systems without renewable generation. A co-optimization of generation and storage expansion decisions for renewable-dominated microgrids is proposed in [37]. The common caveat of [36] and [37] is that they disregard the ability of energy storage to provide PFR and do not explicitly account for post-contingency states. To the best of the authors' knowledge, co-planning of generation and storage siting and sizing, while explicitly accounting for PFR needs and post-contingency states, has not yet been investigated.

B. Contributions

This paper makes the following contributions:

- 1) It presents a mathematical formulation for coordinated generation and storage expansion, while endogenously modeling PFR constraints in the pre-contingency state and its deployment in post-contingency states for every contingency of generating and storage units.
- 2) The proposed formulation optimizes both siting and sizing decisions on storage that can be scheduled to simultaneously provide spatio-temporal arbitrage and PFR services, thus increasing its value to the system with high penetration levels of renewable generation.
- 3) Comparison of the proposed formulation to the traditional expansion model that accounts only for capacity adequacy. This comparison is performed on an ISO New England test system to emphasize the importance of considering the PFR constraints in expansion studies.

In this paper, we consider a generic electrochemical energy storage, which typically has high charging and discharging efficiencies, flexible response characteristics, and flexible power-to-energy ratio that makes it suitable for various grid support applications [28], [29]. Furthermore, this type of energy storage units does not have geographical or climate restrictions on placement decisions.

II. MODEL

A. Assumptions

This paper makes the following assumptions:

- 1) The demand is inelastic. Thus, maximizing the social welfare is equivalent to minimizing the operating costs.
- 2) Generation offer curves are linear with one block, which is common in planning studies, e.g., [17], [18].
- 3) Network constraints are based on a dc approximation.
- 4) The expansion decisions are optimized for a target year modeled by a set of characteristic days. New generating and storage units can be placed at every bus of the system.
- 5) PFR of conventional generating and storage units is automatic and uses local frequency measurements.
- 6) Contingencies are only associated with generating and storage unit failures. Line failures do not cause instant frequency deviations and, thus, do not normally require PFR. All contingencies are cleared within the one time period, i.e., it is assumed that the system is returned to the day-ahead schedule following the post-contingency state.
- 7) The operating cost of storage is assumed to be negligible and storage capacity decay is uniformly distributed during its lifetime. This is a common assumption in most of the storage investment studies, such as [19]. Note that Section III-C quantifies the effect of the storage degradation characteristic on capacity expansion.

B. Mathematical Formulation

Objective function (1) minimizes the annualized investment costs of storage and generating units, the expected operating costs of conventional generating units and the expected load shed costs in pre- and post-contingency states:

$$\begin{aligned}
 & a \left[\sum_{j \in J^C} \left(C_j^{\text{SE,IN}} s_j^{\text{E,IN}} + C_j^{\text{SP,IN}} s_j^{\text{P,IN}} \right) \right. \\
 & + \sum_{g \in \{G^{\text{C,C}} \cup G^{\text{C,I}}\}} C_g^{\text{G,IN}} g_g^{\text{IN}} \left. \right] + \sum_{\omega \in \Omega} \pi_{\omega} \sum_{d \in D} W_d \sum_{t \in T_d} \left[\sum_{g \in G} C_g^{\text{G}} g_{gt\omega} \right. \\
 & \left. + \sum_{n \in N} \left(C^{\text{UD}} p_{nt\omega}^{\text{UD}} + \sum_{k \in K} \tau_k C^{\text{UD,PC}} p_{nt\omega k}^{\text{UD,PC}} \right) \right] \quad (1)
 \end{aligned}$$

As in [13] and [14], the annualized investment costs are calculated based on the capital recovery factor as $a = \frac{r(1+r)^x}{(1+r)^x - 1}$ with interest rate r and lifetime x [38]. This factor allows conversion of the present total investment cost into a stream of equal annual payments over the investment lifetime at a specified interest rate. The objective function is constrained as follows:

1) *Pre-Contingency State Constraints:*

$$0 \leq g_{gt\omega} \leq G_g^{\max}, \quad \forall g \in G^{E,C}, d \in D, t \in T_d, \omega \in \Omega \quad (2)$$

$$0 \leq g_{gt\omega} \leq g_g^{\text{IN}}, \quad \forall g \in G^{C,C}, d \in D, t \in T_d, \omega \in \Omega \quad (3)$$

$$g_{gt\omega} - g_{gt-1,\omega} \leq G_g^{\text{up}}, \\ \forall g \in \{G^{E,C} \cup G^{C,C}\}, d \in D, \{t, t-1\} \in T_d, \omega \in \Omega \quad (4)$$

$$g_{gt-1,\omega} - g_{gt\omega} \leq G_g^{\text{dw}}, \\ \forall g \in \{G^{E,C} \cup G^{C,C}\}, d \in D, \{t, t-1\} \in T_d, \omega \in \Omega \quad (5)$$

$$g_{gt\omega} + g_{gt\omega}^S = U_{gt\omega}^I G_g^{\max}, \\ \forall g \in G^{E,I}, d \in D, t \in T_d, \omega \in \Omega \quad (6)$$

$$g_{gt\omega} + g_{gt\omega}^S = U_{gt\omega}^I g_g^{\text{IN}}, \\ \forall g \in G^{C,I}, d \in D, t \in T_d, \omega \in \Omega \quad (7)$$

$$0 \leq g_g^{\text{IN}} \leq G_g^{\text{IN}}, \quad \forall g \in \{G^{C,C} \cup G^{C,I}\} \quad (8)$$

$$s_{jt\omega} = s_{jt-1,\omega} + \left(\eta_j^S s_{jt\omega}^C - \frac{1}{\eta_j^S} s_{jt\omega}^D \right), \\ \forall j \in J^C, d \in D, t \in T_d, \omega \in \Omega \quad (9)$$

$$\gamma_j^{\min} s_j^{\text{E,IN}} \leq s_{jt\omega} \leq s_j^{\text{E,IN}}, \\ \forall j \in J^C, d \in D, t \in T_d, \omega \in \Omega \quad (10)$$

$$0 \leq s_{jt\omega}^C \leq s_j^{\text{P,IN}}, \quad \forall j \in J^C, d \in D, t \in T_d, \omega \in \Omega \quad (11)$$

$$0 \leq s_{jt\omega}^D \leq s_j^{\text{P,IN}}, \quad \forall j \in J^C, d \in D, t \in T_d, \omega \in \Omega \quad (12)$$

$$s_{jt\omega} = \gamma_j^0 s_j^{\text{E,IN}}, \quad \forall j \in J^C, d \in D, t \in T_d^0, \omega \in \Omega \quad (13)$$

$$s_{jt\omega} \geq \gamma_j^0 s_j^{\text{E,IN}}, \quad \forall j \in J^C, d \in D, t \in T_d^L, \omega \in \Omega \quad (14)$$

$$0 \leq s_j^{\text{E,IN}} \leq S^{\text{IE,max}}, \quad \forall j \in J^C \quad (15)$$

$$p_{\ell t\omega}^L = \frac{1}{X_\ell} (\theta_{O(\ell)t\omega} - \theta_{F(\ell)t\omega}), \\ \forall \ell \in L, d \in D, t \in T_d, \omega \in \Omega \quad (16)$$

$$-P_\ell^{\text{L,max}} \leq p_{\ell t\omega}^L \leq P_\ell^{\text{L,max}}, \\ \forall \ell \in L, d \in D, t \in T_d, \omega \in \Omega \quad (17)$$

$$\sum_{g \in G_n} g_{gt\omega} + \sum_{j \in J_n^C} (s_{jt\omega}^D - s_{jt\omega}^C) - \sum_{\ell \in L_n^O} p_{\ell t\omega}^L + \sum_{\ell \in L_n^F} p_{\ell t\omega}^L \\ + p_{nt\omega}^{\text{UD}} = D_{nt\omega}, \quad \forall n \in N, d \in D, t \in T_d, \omega \in \Omega \quad (18)$$

Constraints (2) and (3) enforce power output limits of the existing and the newly installed conventional generating units. Ramp rate limits on these generating units are enforced in (4) and (5). Power outputs of the existing and the newly installed renewable generating units are limited in (6) and (7). These outputs are subject to parameter $U_{gt\omega}^I \in \{0, 1\}$, which determines the available capacity of renewable unit g during period t and under scenario ω . Constraint (8) limits the maximum capacity of the conventional and renewable units that can be installed. The state of charge of storage is computed in (9) and constrained in (10).

Constraints (11) and (12) limit the charging and discharging power. The storage state of charge at the beginning and at the end of each day is related in (13) and (14), respectively. The maximum energy capacity of storage to be installed is limited in (15). Constraint (16) computes line power flows, which are bounded in (17). The power balance is enforced for every bus in (18) and includes injections of storage candidates placed at bus n . Note that set J_n^C relates storage candidate j and its network location at bus n . Since (18) is enforced $\forall n \in N$, storage can be placed at any bus where it is economically justified.

2) *Post-Contingency State Constraints:*

$$g_{gt\omega k}^{\text{PC}} \geq U_{gk}^{\text{PC}} z_{gt\omega k}^G G_g^{\max}, \\ \forall g \in G^{E,C}, d \in D, t \in T_d, \omega \in \Omega, k \in K \quad (19)$$

$$g_{gt\omega k}^{\text{PC}} \geq U_{gk}^{\text{PC}} z_{gt\omega k}^G g_g^{\text{IN}}, \\ \forall g \in G^{C,C}, d \in D, t \in T_d, \omega \in \Omega, k \in K \quad (20)$$

$$g_{gt\omega k}^{\text{PC}} \leq U_{gk}^{\text{PC}} (g_{gt\omega} - D_g^G \Delta f_{t\omega k}), \\ \forall g \in \{G^{E,C} \cup G^{C,C}\}, d \in D, t \in T_d, \omega \in \Omega, k \in K \quad (21)$$

$$g_{gt\omega k}^{\text{PC}} \geq U_{gk}^{\text{PC}} (g_{gt\omega} - D_g^G \Delta f_{t\omega k}) - U_{gk}^{\text{PC}} M^G z_{gt\omega k}^G, \\ \forall g \in \{G^{E,C} \cup G^{C,C}\}, d \in D, t \in T_d, \omega \in \Omega, k \in K \quad (22)$$

$$0 \leq g_{gt\omega k}^{\text{PC}} \leq U_{gk}^{\text{PC}} G_g^{\max}, \\ \forall g \in G^{E,C}, d \in D, t \in T_d, \omega \in \Omega, k \in K \quad (23)$$

$$0 \leq g_{gt\omega k}^{\text{PC}} \leq U_{gk}^{\text{PC}} g_g^{\text{IN}}, \\ \forall g \in G^{C,C}, d \in D, t \in T_d, \omega \in \Omega, k \in K \quad (24)$$

$$g_{gt\omega k}^{\text{PC}} = U_{gk}^{\text{PC}} g_{gt\omega}, \\ \forall g \in \{G^{C,I} \cup G^{E,I}\}, d \in D, t \in T_d, \omega \in \Omega, k \in K \quad (25)$$

$$s_{jt\omega k}^{\text{D,PC}} \leq (s_{jt-1,\omega} - \gamma_j^{\min} s_j^{\text{IN}}) \eta_j^S, \\ \forall j \in J^C, d \in D, t \in T_d, \omega \in \Omega, k \in K \quad (26)$$

$$s_{jt\omega k}^{\text{D,PC}} \leq V_{jk}^{\text{PC}} s_j^{\text{P,IN}}, \\ \forall j \in J^C, d \in D, t \in T_d, \omega \in \Omega, k \in K \quad (27)$$

$$s_{jt\omega k}^{\text{C,PC}} \leq V_{jk}^{\text{PC}} s_j^{\text{P,IN}}, \\ \forall j \in J^C, d \in D, t \in T_d, \omega \in \Omega, k \in K \quad (28)$$

$$-\Delta f^{\max} \leq \Delta f_{t\omega k} \leq \Delta f^{\max}, \\ \forall d \in D, t \in T_d, \omega \in \Omega, k \in K \quad (29)$$

$$p_{\ell t\omega k}^{\text{L,PC}} = \frac{1}{X_\ell} (\theta_{O(\ell)t\omega k}^{\text{PC}} - \theta_{F(\ell)t\omega k}^{\text{PC}}), \\ \forall \ell \in L, d \in D, t \in T_d, \omega \in \Omega, k \in K \quad (30)$$

$$\sum_{g \in G_n} g_{gt\omega k}^{\text{PC}} + \sum_{j \in J_n^C} (s_{jt\omega k}^{\text{D,PC}} - s_{jt\omega k}^{\text{C,PC}}) - \sum_{\ell \in L_n^O} p_{\ell t\omega k}^{\text{L,PC}} \\ + \sum_{\ell \in L_n^F} p_{\ell t\omega k}^{\text{L,PC}} + p_{nt\omega k}^{\text{UD}} + p_{nt\omega k}^{\text{UD,PC}} = D_{nt\omega}, \\ \forall n \in N, d \in D, t \in T_d, \omega \in \Omega, k \in K \quad (31)$$

In this paper we consider the N-1 security criterion. Therefore, all possible N-1 contingencies on generating and energy storage units are considered at each time period and for each scenario. Given N_G generating and N_J storage units, N_D characteristic days with 24 hourly intervals and N_Ω scenarios at each day, the total number of contingencies considered, while optimizing generation and storage expansion decisions, is $(N_G + N_J) \cdot N_D \cdot 24 \cdot N_\Omega$. Considering this, constraints (19)–(24) model PFR constraints of conventional units. In these constraints, binary variable z_{gtwk}^G indicates whether a generating unit reaches its maximum capacity in the post-contingency state in period t under scenario w in case of contingency k or not. Thus, if binary variable $z_{gtwk}^G = 1$, the post-contingency power output of generating unit g is at its maximum. As a result, (19) and (23) set g_{gtwk}^{PC} to G_g^{max} for the existing generating units, while (20) and (24) set g_{gtwk}^{PC} to g_g^{IN} for the newly built generating units. On the other hand, if $z_{gtwk}^G = 0$, i.e., generating unit g produces below its maximum capacity, (21) and (22) set g_{gtwk}^{PC} to $U_{gk}^{PC}(g_{gtw} - D_g^G \Delta f_{twk})$. Since renewable units do not participate in PFR, constraint (25) keeps the output of both the existing and the newly installed renewable units at their pre-contingency values. Constraint (26) models PFR of storage assuming that storage can discharge all available energy when a contingency happens. Constraints (27) and (28) limit discharging and charging power of storage units. The post-contingency frequency deviation from the nominal value is constrained in (29). Constraints (30)–(31) are post-contingency equivalents of pre-contingency constraints (16)–(18). Note that (20) is nonlinear due to the product of z_{gtwk}^G and g_g^{IN} , which can be linearly reformulated as:

$$g_{gtwk}^{PC} \geq U_{gk}^{PC} x_{gtwk}^{G,I}, \quad \forall g \in G^{C,C}, d \in D, t \in T_d, \omega \in \Omega, k \in K \quad (32)$$

$$0 \leq x_{gtwk}^{G,I} \leq G_g^{IN} z_{gtwk}^G, \quad \forall g \in G^{C,C}, d \in D, t \in T, \omega \in \Omega, k \in K \quad (33)$$

$$g_g^{IN} - G_g^{IN} (1 - z_{gtwk}^G) \leq x_{gtwk}^{G,I} \leq g_g^{IN}, \quad \forall g \in G^{C,C}, d \in D, t \in T_d, \omega \in \Omega, k \in K \quad (34)$$

Given the linearization scheme described in (32)–(34), the proposed optimization is given by:

$$\text{Equations (1) – (19), (21) – (34)}. \quad (35)$$

Problem (35) is a mixed-integer linear program that can be solved by off-the-shelf optimization solvers.

C. Traditional Generation and Storage Expansion Problem

The proposed formulation is numerically compared against a generation and storage expansion problem, based on [16] and [37], that ignores contingencies. Comparison of the proposed and traditional formulations will reveal the effects of including PFR constraints in the planning stage. The traditional generation

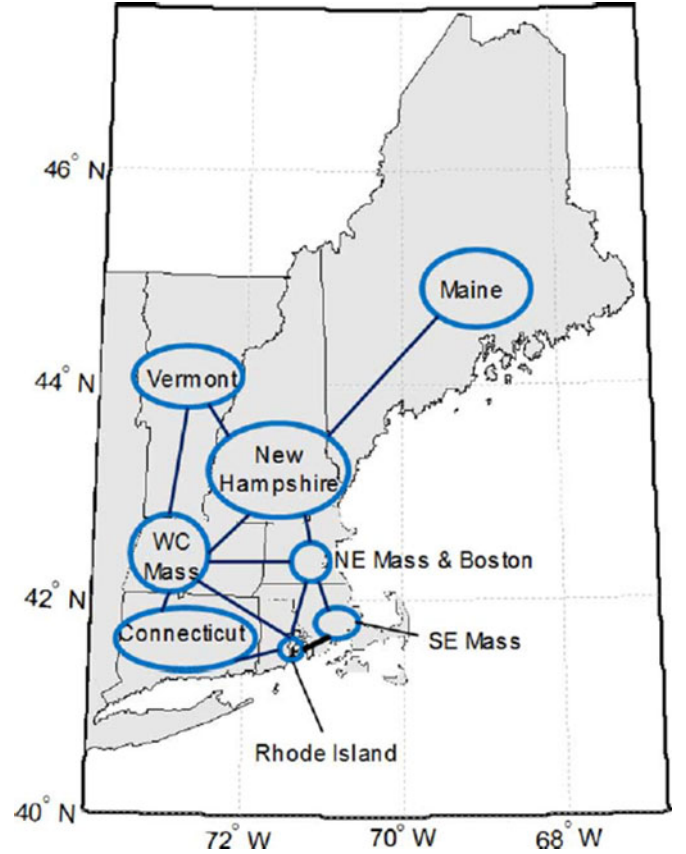


Fig. 1. A diagram of the ISO New England system described in [39].

and storage expansion formulation is given as follows:

Minimize $_{\Theta}$

$$a \left[\sum_{j \in J^C} (C_j^{SE,IN} s_j^{E,IN} + C_j^{SP,IN} s_j^{P,IN}) + \sum_{g \in \{G^{C,C} \cup G^{C,I}\}} C_g^{G,IN} g_g^{IN} \right] + \sum_{\omega \in \Omega} \pi_{\omega} \sum_{d \in D} W_d \times \sum_{t \in T_d} \left[\sum_{g \in G} C_g^G g_{gtw} + \sum_{n \in N} (C^{UD} p_{ntw}^{UD}) \right] \quad (36)$$

Subject to:

$$\text{Constraints (2) – (18)}. \quad (37)$$

III. CASE STUDY

The problem in (35) is tested on an 8-zone model of the ISO New England system [39] illustrated in Fig. 1, where each zone is modeled as a single bus. Annual wind generation profiles with an hourly resolution are taken from [40] for the 30% wind penetration level in terms of annual electricity produced. The target year is represented by a set of characteristic days divided into hourly periods. The characteristic days and weights are selected using the fast-forward scenario reduction algorithm described in [42]. The objective of this algorithm is to represent the original set of 365 days with a reduced set of characteristic days that are close to the days in the original set in terms of

TABLE I
GENERATING UNITS DATA

Technology	Existing capacity (MW)	Candidate capacity (MW)	Investment cost (\$/kW)	Forced outage rate (%)
Nuclear	2,479.0	2,185.9	3,000	4
Coal	294.2	2,101.3	1,650	6
Oil	404.0	4,902.6	750	3
Gas	0.0	12,084.3	750	3
Wind	4,839.5	0.0	1,500	-

the Kantorovich distance. The algorithm is a greedy process that selects one day at each iteration, which minimizes the Kantorovich distance between the reduced and the original set. The iterations are repeated until a specified number of days or a certain probability distance is achieved. Finally, the algorithm computes the weights for the selected characteristic days. Our numerical experiments with different numbers of characteristic days suggest that at least five characteristic days are necessary to ensure numerical stability of the optimal solution of (35). Therefore, these five characteristic days are considered in the experiments below. On each characteristic day, wind power generation is represented using three (average, high and low) scenarios with probabilities of 0.6, 0.2 and 0.2, as customarily done in other planning studies [13], [14]. The average scenario is equal to the wind generation profile provided in [40], whereas the high and low scenarios are obtained by multiplying the average scenario by 1.25 and 0.75. This three-scenario-based representation makes it possible to capture spatial and temporal correlations among wind and wind-demand data, while ensuring computational tractability [13], [14].

We assume that renewable generation investments are fixed by policy mandates and optimize investments in a set of conventional generating technologies and energy storage. Table I provides relevant input data of existing and candidate generating units. The investment costs and forced outage rates of generating units included in Table I are obtained from [43] and [44], respectively. Additionally, the droop is set to 5% and the maximum allowed frequency deviation is 600 mHz. Storage candidate locations are not pre-defined and up to 1000 MW of storage power capacity can be placed at each bus. The maximum charging/discharging duration is set to $\gamma^{\text{EP}} = 6$ hours, i.e., $s_j^{\text{E,IN}} = \gamma^{\text{EP}} s_j^{\text{P,IN}}, \forall j$.¹ The charging and discharging efficiencies of storage units are each 0.95 [30]. The initial and minimum state of charge values of the storages are 0.4 and 0, respectively. The forced outage rate of storage is set to 2% [44]. We analyze three capital cost scenarios of energy storage [19]: low (\$20/kWh and \$500/kW), medium (\$40/kWh and \$1000/kW)

¹The value of $\gamma^{\text{EP}} = 6$ hours is consistent with technical capabilities of prospective storage technologies that are expected to provide spatio-temporal arbitrage [30] and with the needs of systems with high penetration levels of renewable generation in energy spatio-temporal arbitrage services [45]. This assumption can be revisited by enforcing inequality condition $s_j^{\text{E,IN}} \leq \gamma^{\text{EP}} \cdot s_j^{\text{P,IN}}, \forall j$. This modification will not change the problem structure and solution approach, but will make it possible to optimize the maximum charging/discharging in the range from 0 to γ^{EP} hours.

TABLE II
INVESTMENT AND EXPECTED OPERATING COSTS WITH AND WITHOUT
PRIMARY FREQUENCY RESPONSE (PFR) IN THE PLANNING STAGE

Storage cost	Metric	Without PFR	With PFR
High	Investment cost, M \$	1,226.0	1,217.5
	Expected operating cost, M \$	1,488.7	1,497.8
Medium	Investment cost, M \$	1,231.2	1,224.2
	Expected operating cost, M \$	1,475.2	1,484.3
Low	Investment cost, M \$	1,204.3	1,208.3
	Expected operating cost, M \$	1,469.1	1,477.4

and high (\$80/kWh and \$2000/kW). The interest rate and life-time period are set to 5% and 20 years, which yields the capital recovery factor of 8.02%.

All simulations are performed with CPLEX 12.6.1 using a server with ten 2.9 GHz processors and 250 GB of RAM. The optimality gap is set to 0.05%.

A. Effect of PFR Constraints on Expansion Decisions

This section compares the expansion decisions made by the models with (Section II-B) and without (Section II-C) considering the PFR constraints in the planning stage. The difference between these cases reveal the effect of modeling PFR in post-contingency states on the optimal investments. To isolate the effect of the PFR constraints, in this section PFR is only provided by conventional generating units. Since the model in Section II-C does not account for contingencies, we evaluate the expansion decisions made by the model in Section II-C using the model in Section II-B. To this end, the model in Section II-B is re-solved with fixed expansion decisions obtained with the model in Section II-C. Table II displays the investment and operating cost for each case and different capital cost scenarios of storage, while Fig. 2 itemizes the expansion decisions for each technology considered.

Including PFR constraints in the planning stage reduces the investment cost. Since storage units do not provide PFR in this case, the optimization installs other generating units capable of providing PFR and that have lower capital costs. As a result, installed capacity of storage units decreases, which leads to a reduction of the investment cost. Furthermore, generating units capable of providing PFR, which are installed instead of storage units, have a lower capital cost than storage units.

The installed storage capacity monotonically increases as the capital cost of the storage decreases. Under the high capital cost scenario, energy storage is not installed in either of the cases. Modelling PFR in the planning stage reduces the investment cost by 8.5 M\$ (0.69%) and the total capacity of new generating units by 49.9 MW (0.39%). However, this modest change in the total investment cost and capacity leads to a qualitative shift in expansion decisions. Thus, considering PFR reduces the installed capacity of nuclear, coal, and gas units by 62.3 MW (3.82%), 96.5 MW (7.1%), and 54 MW (0.56%), respectively, while the installed capacity of oil units is increased by 162.9 MW (13.0%). This difference can be explained by a relatively low capital cost and outage rate of oil units, as shown in Table I. However, these

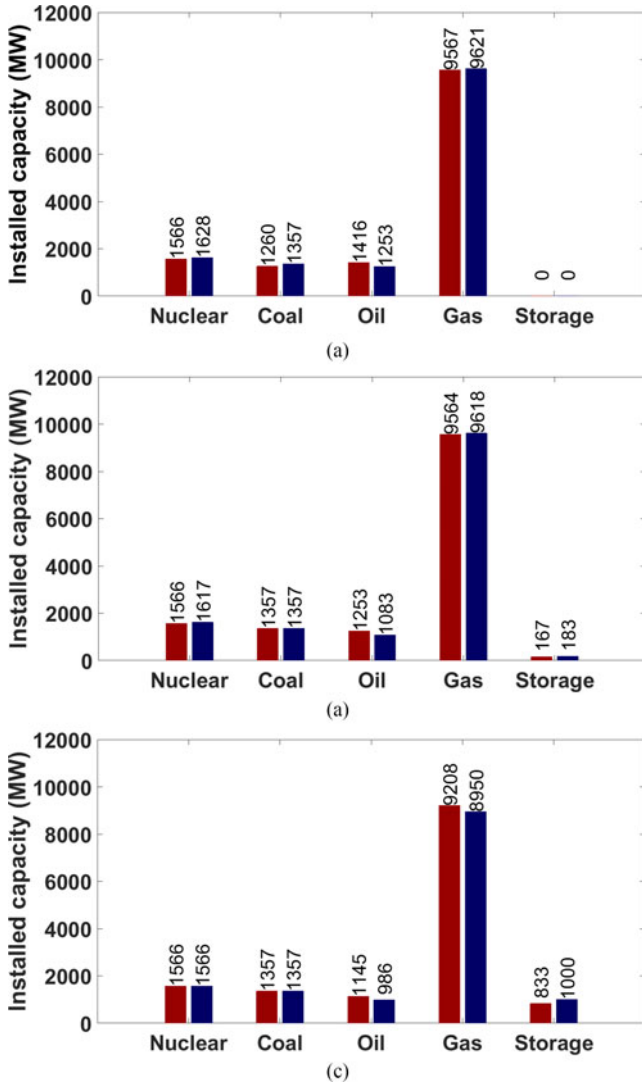


Fig. 2. Expansion decisions with (red) and without (blue) PFR in the planning stage. (a) High cost of storage. (b) Medium cost of storage. (c) Low cost of storage.

units have a relatively high operating cost resulting in an increase of the expected operating cost by 9.1 M\$ (0.61%) if the PFR constraints are modelled in the planning stage.

As the capital cost of energy storage reduces, these units are installed in addition to the conventional generating units and perform spatio-temporal energy arbitrage only. The lower the capital cost, the more energy storage that replaces the capacity of conventional units is installed. Considering the PFR constraints in the planning stage reduces the total power and energy capacity of energy storage installed under both the medium and low capital cost scenarios. Notably, under the low capital cost scenario, modeling of the PFR constraints in the planning stage increases the total investment cost by 4.0 M\$ (0.33%), which contrasts with a reduction of the total investment cost in case of the high and medium capital costs of storage. Also, energy storage deployment under the low capital cost reduces expansion decisions on flexible oil and gas generating units by 158.7 MW (16.1%) and 258.2 MW (2.9%), respectively, while planning

TABLE III
IN-SAMPLE COMPARISON OF POST-CONTINGENCY STATES WITH AND WITHOUT PRIMARY FREQUENCY RESPONSE (PFR) IN THE PLANNING STAGE

Storage cost	Metric	Without PFR	With PFR
High	# of contingencies	7,722	7,459
	% of contingencies with unserved demand	5.335	4.585
	Expected unserved demand, MWh	1,531.7	1,214.5
Med	# of contingencies	8,148	7,666
	% of contingencies with unserved demand	5.167	4.696
	Expected unserved demand, MWh	1,539.9	1,252.4
Low	# of contingencies	8,482	8,476
	% of contingencies with unserved demand	5.423	5.309
	Expected unserved demand, MWh	3,549.4	1,665.7

TABLE IV
PRE- AND POST-CONTINGENCY COSTS WITH AND WITHOUT PRIMARY FREQUENCY RESPONSE (PFR) IN THE PLANNING STAGE

Storage cost	Metric	Without PFR	With PFR
High	Pre-contingency cost, M \$	2,714.7	2,715.3
	Post-contingency cost, M \$	15.3	12.1
	Total cost, M \$	2,730.0	2,727.5
Medium	Pre-contingency cost, M \$	2,706.4	2,708.5
	Post-contingency cost, M \$	15.4	12.5
	Total cost, M \$	2,721.8	2,721.0
Low	Pre-contingency cost, M \$	2,673.4	2,685.7
	Post-contingency cost, M \$	35.5	16.7
	Total cost, M \$	2,708.9	2,702.4

decisions on inflexible nuclear and coal generating units remain unchanged.

Table III presents the in-sample comparison of the planning decisions described in Table II and Fig. 2. This comparison runs day-ahead unit commitment simulations with randomized contingencies and wind power outputs to the system performance during the course of the target year. To avoid miscalculating the percentage of contingencies with unserved demand, contingencies at a) non-installed units, b) off-line generating units, and c) standby (not charging/discharging) storage units are not accounted for in this table. Since less generating and storage units are installed when the PFR constraints are considered, the total number of possible contingencies is reduced by 263 (3.4%), 482 (5.9%), and 6 (0.71%) for the high, medium, and low storage capital cost scenarios, respectively. This reduction leads to a lower occurrence and expected value of unserved demand for all capital costs. Note that even a modest reduction by 6 (0.71%) contingencies, which is observed when the PFR constraints are considered in the planning stage under the low capital cost scenario, reduces the expected unserved demand by 1883.7 MWh (53.1%).

As it can be seen from the numerical results above, considering PFR constraints in the investment model leads to a relatively moderate change in the investment and expected operating costs (Table II), but sizably affects expansion decisions (Fig. 2) and post-contingency performance of the system (Table III).

Table IV includes the pre- and post-contingency costs with and without PFR in the planning stage. In this table

TABLE V
INVESTMENT AND EXPECTED OPERATING COSTS WITH PRIMARY FREQUENCY RESPONSE (PFR) PROVIDED BY CONVENTIONAL GENERATING AND STORAGE UNITS IN THE PLANNING STAGE

Storage cost	Metric	Storage provides PFR	Δ
High	Investment cost, M \$	1,217.5	0
	Expected operating cost, M \$	1,497.8	0
Medium	Investment cost, M \$	1,226.7	2.5
	Expected operating cost, M \$	1480.8	-3.5
Low	Investment cost, M \$	1,212.0	3.7
	Expected operating cost, M \$	1,463.8	-20.4

TABLE VI
EXPANSION DECISIONS WITH PRIMARY FREQUENCY RESPONSE (PFR) PROVIDED BY GENERATORS AND STORAGE IN THE PLANNING STAGE

Storage cost	Technology	Storage provides PFR	Δ
High	Nuclear, MW	1,565.7	0
	Coal, MW	1,260.4	0
	Oil, MW	1,416.1	0
	Gas, MW	9,566.5	0
	Storage, MW	0	0
	Storage, MWh	0	0
Medium	Nuclear, MW	1,565.7	0
	Coal, MW	1,356.9	0
	Oil, MW	1,225.5	27.9
	Gas, MW	9,516.3	47.7
	Storage, MW	237.7	71.0
	Storage, MWh	1426.1	426.1
Low	Nuclear, MW	1,565.7	0
	Coal, MW	1,356.9	96.5
	Oil, MW	1,006.1	138.5
	Gas, MW	8,959.6	-248.7
	Storage, MW	1,119.3	286.0
	Storage, MWh	6,715.5	1,715.5

pre-contingency cost refers to the sum of the investment and operating costs presented in Table II, whereas post-contingency costs are the expected unserved demand costs. Thus, the pre-contingency costs are smaller in all cases in which PFR is not considered in the planning stage, but at the expense of higher post-contingency costs. As a result, the total costs are smaller when PFR are considered in the planning stage.

B. Effect of Storage Providing PFR on Expansion Decisions

This section compares the expansion decisions made with the PFR constraints considered in the planning stage, as in Section III-A, when provided by conventional generating units only and by both conventional generating units and energy storage. Table V summarizes the investment and operating costs and Table VI itemizes the expansion decisions for each case. Table VII presents the in-sample comparison of the expansion decisions described in Tables V and VI as described in Section II-C. Note that Δ in Tables V–VII denotes the difference to the respective entries in Tables II and III and Fig. 2 with the FPR constraints.

If the capital cost of energy storage remains high, no energy storage is installed and, thus, there is no difference in expansion decisions relative to Section III-A. However, as the capital cost of storage reduces, the investment cost increases by 2.5 (0.20%)

TABLE VII
IN-SAMPLE COMPARISON OF POST-CONTINGENCY STATES WITH PRIMARY FREQUENCY RESPONSE (PFR) PROVIDED BY GENERATORS AND STORAGE IN THE PLANNING STAGE

Storage cost	Metric	Storage provides PFR	Δ
High	# of contingencies	7,459	0
	% of contingencies with unserved demand	4,585	0
	Expected unserved demand, MWh	1,214.5	0
Med	# of contingencies	7,840	134
	% of contingencies with unserved demand	4,247	-0.449
	Expected unserved demand, MWh	1,163.0	-89.4
Low	# of contingencies	8,778	302
	% of contingencies with unserved demand	2,427	-2.882
	Expected unserved demand, MWh	780.9	-884.8

and 3.5 M\$ (0.31%) for the medium and low capital cost scenarios. These investments increase the expected operating cost savings of 3.5 M\$ (0.24%) and 20.4 M\$ (1.38%), respectively. These cost reductions are predominately achieved by the investments in storage which are increased by 71 MW (41.6%) and 286 MW (34.3%), respectively, while the total capacity of conventional units is increased by 75.6 MW (0.55%) for the medium cost scenario and is reduced by 13.7 MW (0.10%) for the low cost scenario. The reduction of the total capacity of conventional units installed under the low capital cost scenario of storage is caused by lower investments in the gas generating units.

Considering the ability of energy storage to provide PFR has a two-fold effect on the in-sample comparison presented in Table VII. First, the total number of possible contingencies increases as compared to the case presented in Section III-A. Second, both the fraction of contingencies that results in unserved demand and the expected value of unserved demand reduce. Notably, these reductions increase as the storage capital cost reduces and more capacity storage is installed. This trend indicates that the ability of energy storage to provide PFR is crucial for future energy storage procurement when capital costs are projected to decrease.

C. Impact of the Degradation Characteristic

This section analyzes the effect of the battery degradation characteristic on the expansion decisions produced by the model in (35). The cost of battery degradation is computed using the linear regression model described in [46], which assumes that the capacity degradation is a linear function of the number of round trip cycles. If N_j^{Cyc} is the number of complete charge/discharge cycles that storage unit j performs over its lifetime, the expected battery degradation cost on characteristic day d under scenario ω can be computed as:

$$c_{jd\omega}^{Deg} = \sum_{t \in T_d} \frac{1}{N_j^{Cyc}} C_j^{SE,IN} \left(s_{jt\omega}^D + \sum_{k \in K} \tau_k \left(s_{jt\omega k}^{D,PC} - s_{jt\omega}^D \right) \right) \quad (38)$$

Note that since the battery degradation is assumed to be a function of the round-trip cycle, constraint (38) implicitly assumes that the energy discharged will be charged back in a future time period.

TABLE VIII

EFFECT OF THE BATTERY DEGRADATION CHARACTERISTIC ON INVESTMENT AND EXPECTED OPERATING COSTS WITH PRIMARY FREQUENCY RESPONSE (PFR) PROVIDED BY GENERATORS AND STORAGE IN THE PLANNING STAGE

Storage cost	Metric	$\Delta\gamma^{\text{Degr}} = 1$	$\Delta\gamma^{\text{Degr}} = 0.8$
Medium	Investment cost, M	0	0.9
	Expected operating cost, M \$	0	1.6
Low	Investment cost, M \$	0	0.3
	Expected operating cost, M \$	0	1.1

TABLE IX

INFLUENCE OF DEGRADATION CHARACTERISTICS ON EXPANSION DECISIONS WITH PRIMARY FREQUENCY RESPONSE (PFR) PROVIDED BY GENERATORS AND STORAGE IN THE PLANNING STAGE

Storage cost	Technology	$\Delta\gamma^{\text{Degr}} = 1$	$\Delta\gamma^{\text{Degr}} = 0.8$
Medium	Nuclear, MW	0	0
	Coal, MW	0	0
	Oil, MW	0	5.54
	Gas, MW	0	11.2
	Storage, MW	0	-19.1
Storage, MWh	0	-114.3	
Low	Nuclear, MW	0	0
	Coal, MW	0	0
	Oil, MW	0	1.8
	Gas, MW	0	-8.0
	Storage, MW	0	14.6
	Storage, MWh	0	87.9

To prevent early aging of storage units, the annual degradation cost should be smaller than the annualized capital cost. In other words, if the battery degradation cost is greater than its capital cost, the battery lifetime will be reduced. Therefore, the annual degradation cost for each storage unit j can be limited as follows:

$$\sum_{d \in D} W_d c_{jd\omega}^{\text{Deg}} \leq \gamma^{\text{Degr}} \left(a C_j^{\text{SE,IN}} \right), \quad \forall j \in J, \omega \in \Omega \quad (39)$$

where γ^{Degr} is a parameter used to control the maximum allowed battery degradation.

Tables VIII and IX summarize the investment and operating costs and the expansion decisions for different values of parameter γ^{Degr} and capital costs of storage when PFR is provided by generating and storage units in the planning stage. Note that Δ in these tables denotes the difference to the result reported in Tables VI and VII, where no battery degradation is considered. Since no energy storage is installed under the high capital cost scenario, this case is not considered in this section. In these simulations, a typical value of $N_j^{\text{Cyc}} = 4500$ cycles has been considered.

If $\gamma^{\text{Degr}} = 1$, the optimal expansion decisions are identical to the case in which storage degradation was not modeled. This means that, under a linear capacity degradation assumption, the resulting usage of the storage units when degradation was not considered will not reduce their lifetime. However, if the usage of the storage units is further limited ($\gamma^{\text{Degr}} = 0.8$) the expansion decisions change accordingly. This results in an increase in the investment and expected operating costs (see Table VIII). Note considering degradation effects strengthens

TABLE X

SENSITIVITY OF THE INVESTMENT AND EXPECTED OPERATING COSTS TO THE COST OF UNSERVED DEMAND (C^{UD}) WITH PRIMARY FREQUENCY RESPONSE (PFR) PROVIDED BY GENERATORS AND STORAGE IN THE PLANNING STAGE

Storage cost	Metric	$C^{\text{UD}}, \cdot 10^3 \text{ \$/MWh}$		
		10	50	100
Low	Investment cost, M \$	1,212.0	1,227.9	1,234.9
	Expected operating cost, M \$	1,463.8	1,460.4	1,460.2

TABLE XI

SENSITIVITY OF THE EXPANSION DECISIONS TO THE COST OF UNSERVED DEMAND (C^{UD}) WITH PRIMARY FREQUENCY RESPONSE (PFR) PROVIDED BY GENERATORS AND STORAGE IN THE PLANNING STAGE

Storage cost	Technology	$C^{\text{UD}}, \cdot 10^3 \text{ \$/MWh}$		
		10	50	100
Low	Nuclear, MW	1,565.7	1,565.7	1,565.7
	Coal, MW	1,356.9	1,356.9	1,356.9
	Oil, MW	1,006.1	1,039.5	1,107.7
	Gas, MW	8,959.6	9,013.2	9,062.3
	Storage, MW	1,119.2	1,333.3	1,333.3
	Storage, MWh	6,715.5	8,000.0	8,000.0

TABLE XII

SENSITIVITY OF THE POST-CONTINGENCY STATES WITH PRIMARY FREQUENCY RESPONSE (PFR) PROVIDED BY GENERATORS AND STORAGE IN THE PLANNING STAGE

Storage cost	Metric	$C^{\text{UD}}, \cdot 10^3 \text{ \$/MWh}$		
		10	50	100
Low	# of contingencies	8,778	8,845	8,873
	% of contingencies with unserved demand	2.427	0.893	0.462
	Expected unserved demand, MWh	780.8	205.8	105.4

the dependency of storage investments on the storage capital cost scenario. Thus, if the storage capital cost is low, the reduction of the usage of the storage units enforced by (39) is compensated by increasing the investments in storage. However, if the storage capital cost is medium, the investments in storage are reduced.

D. Sensitivity to the Cost of Unserved Demand

This section analyzes the impact of the cost of unserved demand (C^{UD}) on the expansion decisions obtained in Section III-B. The investment and operating costs are sensitive to the cost of unserved demand, as shown in Table X. If parameter C^{UD} changes from 10,000 \$/MWh to 100,000 \$/MWh, the investment cost gradually increases, while the operating cost saturates. The increase in the investment cost occurs due to higher installations of flexible oil and gas generators and energy storage, as displayed in Table XI. The installed capacity of nuclear and coal generators remains unaffected if the cost of unserved demand changes. As shown in Table XII, the investments in flexible generating and energy storage units avoid the contingencies that lead to unserved demand and its expected value.

TABLE XIII

INVESTMENT AND EXPECTED OPERATING COSTS WITH PRIMARY FREQUENCY RESPONSE (PFR) PROVIDED BY GAS-ONLY GENERATORS AND STORAGE IN THE PLANNING STAGE

Storage cost	Metric	Storage provides PFR	Δ
High	Investment cost, M \$	1,025.3	-192.2
	Expected operating cost, M \$	1,972.6	474.8
Medium	Investment cost, M \$	1,031.8	-194.9
	Expected operating cost, M \$	1,964.9	484.1
Low	Investment cost, M \$	1,011.9	-200.1
	Expected operating cost, M \$	1,962.7	464.9

TABLE XIV

INVESTMENT AND EXPECTED OPERATING COSTS WITH PRIMARY FREQUENCY RESPONSE (PFR) PROVIDED BY GENERATORS AND STORAGE IN THE PLANNING STAGE

Storage cost	Technology	Storage provides PFR	Δ
High	Gas, MW	17,035.8	7,469.3
	Storage, MW	0	0
	Storage, MWh	0	0
Medium	Gas, MW	16,869.1	7,352.8
	Storage, MW	166.7	-71.0
	Storage, MWh	1,000.	-426.1
Low	Gas, MW	15869.8	6910.2
	Storage, MW	1,166.2	280.7
	Storage, MWh	6,996.2	46.7

The reductions are achieved while a number of contingencies increases for higher values of C^{UD} due to a greater number of generators installed.

E. Effect of Gas-Only Generation Expansion

The availability and relatively low prices of natural gas has led to its increased use for electricity generation, while investments in coal and nuclear generating units have been kept at minimum [41]. In this subsection we study how the expansion decisions with storage providing PFR reported in Section III-B change if gas-fired generating units is the only conventional generation technology available. Table XIII and XIV summarize the investment and operating costs and itemize the expansion decisions for each case, where parameter Δ denotes the difference with respect to the results in Tables VI and VII.

In case of gas-only generation expansion, the total investment cost reduces as compared to the case when investments in other generation technologies are available. These reductions monotonically increase as the capital cost of energy storage decreases. As a result of lower investment costs, the expected operating costs increase for higher storage capital costs. It is noteworthy that, similarly to the results in Table VI, energy storage is not installed under the high capital cost of storage in case of gas-only generation expansion. Since gas generating units are flexible resources, the in-sample comparison presented in Table XV demonstrates that the frequency of the unserved demand occurrences and its expected values reduce for all storage capital cost scenarios.

TABLE XV

IN-SAMPLE COMPARISON OF POST-CONTINGENCY STATES WITH PRIMARY FREQUENCY RESPONSE (PFR) PROVIDED BY GAS-ONLY GENERATORS AND STORAGE IN THE PLANNING STAGE

Storage cost	Metric	Storage provides PFR	Δ
High	# of contingencies	7,109	-350
	% of contingencies with unserved demand	3.882	-0.703
	Expected unserved demand, MWh	933.4	-281.1
Med	# of contingencies	7,337	-503
	% of contingencies with unserved demand	3.789	-0.458
	Expected unserved demand, MWh	914.0	-249.0
Low	# of contingencies	7,649	-1129
	% of contingencies with unserved demand	3.831	-1.404
	Expected unserved demand, MWh	897.9	-117.0

TABLE XVI
COMPUTING TIMES (HOURS)

Storage cost	Section III-A		Section III-B
	Without PFR	With PFR	Storage provides PFR
High	0.5	39.4	66.1
Med	0.6	34.0	72.9
Low	0.6	33.6	71.2

F. Computational Performance

Table XVI presents computing times required to solve each case reported in Sections III-A and III-B with 5 characteristic days and 3 renewable generation scenarios for each day. As shown in Table XVI, the effect of considering the PFR constraints in the planning stage increases computing times (roughly, by two orders of magnitude). The inclusion of the PFR provided by energy storage in the planning stage introduces additional constraints and variables to the problem and, thus, also increases computing times. However, the maximum computing time per instance (72.9 hours) remains acceptable for planning models. In general, computational performance of the proposed planning model is sensitive to the number of characteristic days. However, our experiments indicate that 5 characteristic days ensure numerical stability of the optimal expansion decisions.

IV. CONCLUSION

This paper presents a coordinated generation and storage expansion formulation that explicitly accounts for the PFR constraints in the planning stage. The model is analyzed on a ISO New England test system and compared to the traditional benchmark. The case study considers different energy storage capital costs scenarios and availability of conventional generating units. Based on the numerical results presented in the case study, the following conclusions can be made:

- 1) Considering PFR constraints at the planning stage changes expansion decisions on conventional generating and energy storage units;
- 2) It also reduces the frequency and expected value of the unserved demand;

- 3) The value of energy storage to the system can be increased if it is scheduled to provide PFR services in addition to performing spatio-temporal energy arbitrage.

REFERENCES

- [1] E. Ela and M. O'Malley, "Studying the variability and uncertainty impacts of variable generation at multiple timescales," *IEEE Trans. Power Syst.*, vol. 27, no. 3, pp. 1324–1333, Aug. 2012.
- [2] Y. V. Makarov, C. Loutan, M. Jian, and P. de Mello, "Operational impacts of wind generation on California power systems," *IEEE Trans. Power Syst.*, vol. 24, no. 2, pp. 1039–1050, May 2009.
- [3] E. Lannoye, D. Flynn, and M. O'Malley, "Evaluation of power system flexibility," *IEEE Trans. Power Syst.*, vol. 27, no. 2, pp. 922–931, May 2012.
- [4] Y. Dvorkin, D. S. Kirschen, and M. A. Ortega-Vazquez, "Assessing flexibility requirements in power systems," *IET Gener., Transmiss. Distrib.*, vol. 8, pp. 1820–1830, 2014.
- [5] E. Muljadi, V. Gevorgian, M. Singh, and S. Santoso, "Understanding inertial and frequency response of wind power plants," in *Proc. 2012 IEEE Power Electron. Mach. Wind Appl.*, Denver, CO, USA, Jul. 2012, pp. 1–8.
- [6] Y. Wang, G. Delille, H. Bayem, X. Guillaud, and B. Francois, "High wind power penetration in isolated power systems—assessment of wind inertial and primary frequency responses," *IEEE Trans. Power Syst.*, vol. 28, no. 3, pp. 2412–2420, Aug. 2013.
- [7] H. Ye, W. Pei, and Z. Qi, "Analytical modeling of inertial and droop responses from a wind farm for short-term frequency regulation in power systems," *IEEE Trans. Power Syst.*, vol. 31, no. 5, pp. 3414–3423, Sep. 2016.
- [8] E. Sáiz-Marín, J. García-González, J. Barquín, and E. Lobato, "Economic assessment of the participation of wind generation in the secondary regulation market," *IEEE Trans. Power Syst.*, vol. 27, no. 2, pp. 866–874, May 2012.
- [9] Y. Dvorkin, M. A. Ortega-Vazquez, and D. S. Kirschen, "Wind generation as a reserve provider," *IET Gener., Transmiss. Distrib.*, vol. 9, no. 8, pp. 779–787, May 2015.
- [10] M. Hedayati-Mehdiabadi, J. Zhang, and K. W. Hedman, "Wind power dispatch margin for flexible energy and reserve scheduling with increased wind generation," *IEEE Trans. Sustain. Energy*, vol. 6, no. 4, pp. 1543–1552, Oct. 2015.
- [11] D. Eager, B. F. Hobbs, and J. W. Bialek, "Dynamic modeling of thermal generation capacity investment: Application to markets with high wind penetration," *IEEE Trans. Power Syst.*, vol. 27, no. 4, pp. 2127–2137, Nov. 2012.
- [12] J. Ma, V. Silva, R. Belhomme, D. S. Kirschen, and L. F. Ochoa, "Evaluating and planning flexibility in sustainable power systems," *IEEE Trans. Sustain. Energy*, vol. 4, no. 1, pp. 200–209, Jan. 2013.
- [13] R. Domínguez, A. J. Conejo, and M. Carrión, "Toward fully renewable electric energy systems," *IEEE Trans. Power Syst.*, vol. 30, no. 1, pp. 316–326, Jan. 2015.
- [14] R. Domínguez, A. J. Conejo, and M. Carrión, "Investing in generation capacity: A multi-stage linear-decision-rule approach," *IEEE Trans. Power Syst.*, vol. 31, no. 6, pp. 4784–4794, Nov. 2016.
- [15] L. Baringo and A. J. Conejo, "Risk-constrained multi-stage wind power investment," *IEEE Trans. Power Syst.*, vol. 28, no. 1, pp. 401–411, Feb. 2013.
- [16] D. Pudjianto, M. Aunedi, P. Djapic, and G. Strbac, "Whole-systems assessment of the value of energy storage in low-carbon electricity systems," *IEEE Trans. Smart Grid*, vol. 5, no. 2, pp. 1098–1109, Mar. 2014.
- [17] K. Dvijotham, M. Chertkov, and S. Backhaus, "Storage sizing and placement through operational and uncertainty-aware simulations," in *Proc. 47th Hawaii Int. Conf. Syst. Sci.*, Jan. 2014, pp. 2408–2416.
- [18] Y. Dvorkin, R. Fernández-Blanco, D. S. Kirschen, H. Pandžić, J.-P. Watson, and C. Silva-Monroy, "Ensuring profitability of energy storage," *IEEE Trans. Power Syst.*, vol. 32, no. 1, pp. 611–623, Jan. 2017.
- [19] H. Pandžić, Y. Wang, T. Qiu, Y. Dvorkin, and D. S. Kirschen, "Near-optimal method for siting and sizing of distributed storage in a transmission network," *IEEE Trans. Power Syst.*, vol. 30, no. 5, pp. 2288–2300, Sep. 2015.
- [20] S. Wogrin and D. F. Gayme, "Optimizing storage siting, sizing, and technology portfolios in transmission-constrained networks," *IEEE Trans. Power Syst.*, vol. 30, no. 6, pp. 3304–3313, Nov. 2015.
- [21] J. Ingleson and E. Allen, "Tracking the eastern interconnection frequency governing characteristic," in *Proc. 2010 IEEE Power Eng. Soc. General Meeting*, Jul. 2010, pp. 1–6.
- [22] P. Du and Y. Makarov, "Using disturbance data to monitor primary frequency response for power system interconnections," *IEEE Trans. Power Syst.*, vol. 29, no. 3, pp. 1431–1432, May 2014.
- [23] H. Chavez, R. Baldick, and S. Sharma, "Governor rate-constrained OPF for primary frequency control adequacy," *IEEE Trans. Power Syst.*, vol. 29, no. 3, pp. 1473–1480, May 2014.
- [24] H. Ahmadi and H. Ghasemi, "Security-constrained unit commitment with linearized system frequency limit constraints," *IEEE Trans. Power Syst.*, vol. 29, no. 4, pp. 1536–1545, Jul. 2014.
- [25] Y. Dvorkin, P. Henneaux, D. S. Kirschen, and H. Pandžić, "Optimizing primary response in preventive security-constrained optimal power flow," *IEEE Syst. J.*, to be published.
- [26] T. Thien *et al.*, "Planning of grid-scale battery energy storage systems: Lessons learned from a 5 MW hybrid battery storage project in Germany," RWTH Aachen Univ., Aachen, Germany, Tech. Rep., 2015. [Online]. Available: <https://goo.gl/qgueUz>
- [27] "Enhanced frequency control capability," National Grid, Battery Storage Investigation Report, Tech. Rep., Warwick, U.K., Jun. 2015. [Online]. Available: <https://goo.gl/2ipXey>
- [28] P. F. Ribeiro, B. K. Johnson, M. L. Crow, A. Arsoy, and Y. Liu, "Energy storage systems for advanced power applications," *Proc. IEEE*, vol. 89, no. 12, pp. 1744–1756, Dec. 2001.
- [29] B. Dunn, H. Kamath, and J.-M. Tarascon, "Electrical energy storage for the grid: A battery of choices," *Science*, vol. 334, pp. 928–935, 2011.
- [30] M. Hoffman, A. Sadovsky, M. Kintner-Meyer, and J. DeSteese, "Analysis tools for sizing and placement of energy storage in grid applications: A literature review," Pacific Northwest Nat. Lab., Richland, WA, USA, Tech. Rep. PNNL-19703, Sep. 2010. [Online]. Available: <https://goo.gl/udNWrb>
- [31] T. Borsche, A. Ulbig, M. Koller, and G. Andersson, "Power and energy capacity requirements of storages providing frequency control reserves," in *Proc. 2013 IEEE Power Energy Soc. General Meeting*, Vancouver, BC, Canada, 2013.
- [32] G. Delille, B. Francois, and G. Malarange, "Dynamic frequency control support by energy storage to reduce the impact of wind and solar generation on isolated power system's inertia," *IEEE Trans. Sustain. Energy*, vol. 3, no. 4, pp. 931–939, Oct. 2012.
- [33] V. Knap, S. Chaudhary, D. Stroe, M. Swierczynski, B. Craciun, and R. Teodorescu, "Sizing of an energy storage system for grid inertial response and primary frequency reserve," *IEEE Trans. Power Syst.*, vol. 31, no. 5, pp. 3447–3456, Sep. 2016.
- [34] Y. Zhang, C. Zhao, W. Tang, and S. H. Low, "Profit maximizing planning and control of battery energy storage systems for primary frequency control," *IEEE Trans. Smart Grid*, to be published.
- [35] Y. Wen, C. Guo, H. Pandžić, and D. S. Kirschen, "Enhanced security-constrained unit commitment with emerging utility-scale energy storage," *IEEE Trans. Power Syst.*, vol. 31, no. 1, pp. 652–662, Jan. 2016.
- [36] K. Yasuda, K. Nishiya, J. Hasegawa, and R. Yokoyama, "Optimal generation expansion planning with electric energy storage systems," in *Proc. 14th Annu. Conf. Ind. Electron. Soc.*, Oct. 1988, pp. 550–555.
- [37] E. Hajipour, M. Bozorg, and M. Fotuhi-Firuzabad, "Stochastic capacity expansion planning of remote microgrids with wind farms and energy storage," *IEEE Trans. Sustain. Energy*, vol. 6, no. 2, pp. 491–498, Apr. 2015.
- [38] H. M. Steiner, *Engineering Economic Principles*. Blacklick, OH, USA: McGraw-Hill College, 1988.
- [39] D. Krishnamurthy, W. Li, and L. Tesfatsion, "An 8-zone test system based on ISO New England data: Development and application," *IEEE Trans. Power Syst.*, vol. 31, no. 1, pp. 234–246, Jan. 2016.
- [40] Eastern Wind Dataset, Nat. Renewable Energy Lab., Golden, CO, USA, 2012. [Online]. Available: <https://goo.gl/ZtBFRL>
- [41] R. Levitan, S. Wilmer, and R. Carlson, "Pipeline to reliability: Unraveling gas and electric interdependencies across the eastern interconnection," *IEEE Power Energy Mag.*, vol. 12, no. 6, pp. 78–88, Nov./Dec. 2014.
- [42] N. Gröwe-Kuska, H. Heitsch, and W. Römisich, "Scenario reduction and scenario tree construction for power management problems," in *Proc. IEEE Bologna Power Technol. Conf.*, Bologna, Italy, Jun. 2003.
- [43] Energy Technology Perspectives 2010—Scenarios and Strategies to 2050, International Energy Agency, Paris, France, 2010. [Online]. Available: <https://goo.gl/IA1szN>

- [44] Cost and Performance Data for Power Generation Technologies, Nat. Renewable Energy Lab., Golden, CO, USA, 2012. [Online]. Available: <https://goo.gl/7quPVN>
- [45] R. Fernandez-Blanco, Y. Dvorkin, B. Xu, Y. Wang and D. S. Kirschen, "Optimal energy storage siting and sizing: A WECC case study," *IEEE Trans. Sustain. Energy*, vol. 8, no. 2, pp. 733–743, Apr. 2017.
- [46] M. A. Ortega-Vazquez, "Optimal scheduling of electric vehicle charging and vehicle-to-grid services at household level including battery degradation and price uncertainty," *IET Gener., Transmiss. Distrib.*, vol. 8, no. 6, pp. 1007–1016, 2014.

Miguel Carrión (M'08) received the Ingeniero Industrial and Ph.D. degrees from the Universidad de Castilla-La Mancha, Ciudad Real, Spain, in 2003 and 2008, respectively.

He is currently an Associate Professor at the Universidad de Castilla-La Mancha, Toledo, Spain. His research interests include power systems economics and stochastic programming.

Yury Dvorkin (S'11–M'16) received the Ph.D. degree from the University of Washington, Seattle, WA, USA, in 2016.

He is currently an Assistant Professor in the Department of Electrical and Computer Engineering, New York University, New York, NY, USA. His research interests include short- and long-term planning in power systems with renewable generation and power system economics.

Prof. Dvorkin received the 2016 Scientific Achievement Award by Clean Energy Institute (University of Washington) for his doctoral dissertation "Operations and planning in sustainable power systems."

Hrvoje Pandžić (S'06–M'12) received the M.E.E. and Ph.D. degrees from the Faculty of Electrical Engineering and Computing, University of Zagreb, Zagreb, Croatia, in 2007 and 2011, respectively.

From 2012 to 2014, he was a Postdoctoral Researcher at the University of Washington, Seattle, WA, USA. He is currently an Assistant Professor with the Faculty of Electrical Engineering and Computing, University of Zagreb. His research interests include planning, operation, control, and economics of power and energy systems.